A Multi-Cell Lighting Testbed for VLC and VLP

Thomas Little,* Michael Rahaim,† Iman Abdalla,* Emily Lam,* Richard Mcallister,* Anna Maria Vegni‡
*Electrical and Computer Engineering Department, Boston University, Boston, MA USA
†Engineering Department, University of Massachusetts at Boston, Boston, MA USA
‡Department of Engineering, Roma Tre University, Rome, Italy
tdcl@bu.edu

***Abstract*—Future deployments of LiFi will incorporate arrays of luminaires. We seek to explore the interactions among multiple users, mobility of devices, device orientation, and user traffic. We describe a new multi-cell lighting testbed created to study and optimize dense LiFi systems. The testbed is constructed with 15 commercial LED lights that are driven by custom LiFi drivers and a 16-channel software defined radio. We develop a model for the system for the purpose of predicting signal strength under mobility and different receiver orientations. Data collected in the testbed show good conformance to the model. Lastly, we show how the analytical model and the measured data can be used to study RSS-based VLP and VLC handover in multi-cell systems.**

***Index Terms*—LiFi, multi-cell lighting, visible light communications, visible light positioning, testbeds**

I. Introduction

Recent work in LiFi technology has emphasized the development of very high speed bench-top demonstrations of point-to-point VLC links [1]–[3]. These efforts show the potential to realize data rates in the range of $[1, 10]$ Gbps using Light Emitting Diode (LED) or Laser Device (LD) sources; however, there remain practical issues to realizing these systems in affordable ubiquitous lighting systems.

Considerable work will be required to address optics packaging, connectivity for non-static links, energy consumption and tuning. More realistic solutions with more modest data rates in the $[10, 100]$ Mbps range have been demonstrated and in some cases productized, thus allowing LiFi to be deployed more widely. To be successful, all these emerging systems also need to compete, or at least offer competitive use cases, when challenged by existing WiFi solutions. All of these questions relate both to LiFi (i.e., VLC) and to indoor positioning with visible light positioning (i.e., VLP).

We have set out to identify and understand important design parameters necessary to deploy emerging LiFi alongside of WiFi and emerging mmWave technology. To this end, we have constructed a LiFi (i.e., VLC and VLP) testbed comprised of 15 LED-based luminaires arrayed as a 3×5 dense network and supporting 15 independent LiFi channels, as depicted in Fig. 1. Modulation of luminaires is achieved with an Software Defined Radio (SDR) system based on the Universal Software Radio Peripheral (USRP) hardware [4], [5] with control via GNURadio or Matlab/Simulink software toolkits. The networked configuration of USRPs is capable of supporting 16 baseband channels or 8 passband channels. We build up channel and system models of the testbed and show a comparison of theoretical –*predicted*– performance vs. empirical –*measured*– data in the system. Data are collected to support study of VLP and VLC handover design; we show how receiver position and rotation affect Signal Noise Ratio (SNR) and provide insights on system optimization.

This work was supported in part by the Engineering Research Centers Program of the National Science Foundation under NSF Cooperative Agreement No. EEC-0812056 and by NSF CNS-1617924.

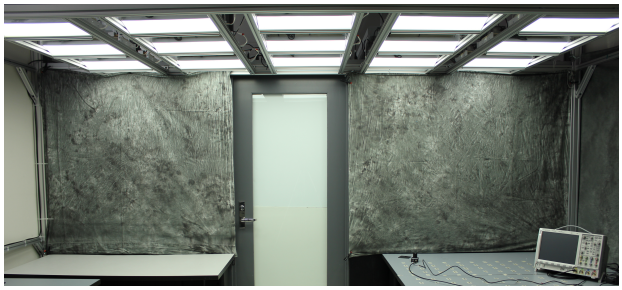

Fig. 1. Multi-Cell Lighting Array Testbed.

The remainder of the paper is organized as follows. Section II describes our VLC/VLP testbed and model. Section III explores Received Signal Strenght (RSS)-based multilateration in a dense array of VLC cells. Section IV considers data collected to influence the design of handover algorithms. Section V concludes the paper.

II. Testbed

The lighting array and testbed environment are illustrated in Fig. 1. The configuration, channel model, and approach to data measurement are described below.

A. Configuration

Fig. 2 shows the physical dimensions of the lighting elements. The luminaires are Cree (#CR22-32L-35K-S) with size of 46×24 cm^2. These are spaced at 50×24 cm^2 on center. Note that the fixtures come packaged in a 2×2 recessed troffer; but the outer shell of each fixture has been removed.

The receiver is configured to move to arbitrary positions on a fixed plane at a distance D_z below the plane of the luminaires. The receiver can also be rotated and tilted to arbitrary angles by servomechanism, while maintaining the same fixed distance to the ceiling. The receiver is a ThorLabs unit (#APD120A2) that can adopt a variety of filters, lenses, and lens tubes to vary the receiver field of view (FOV).

T. Little, M. Rahaim, I. Abdalla, E. Lam, R. Mcallister and A. M. Vegni, "A multi-cell lighting testbed for VLC and VLP," 2018 Global LIFI Congress (GLC), Paris, France, 2018, pp. 1-6, doi: 10.23919/GLC.2018.8319111.

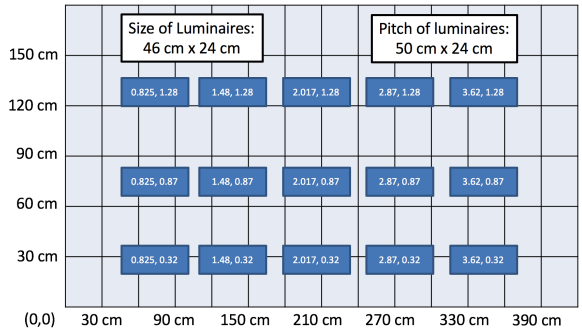

Fig. 2. Layout of Luminaires and Dimensions

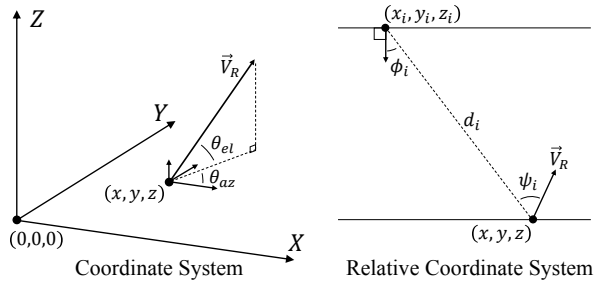

Fig. 3. Geometry and Frames of Reference for Device Orientation.

B. Channel Model

The system geometry is characterized by the coordinate model shown in Fig. 3. Here both the transmitters and receiver are defined in relative terms between the plane of the transmitters and the receiver plane, where mobility, rotation and tilt are experienced. As predicted, changes in the tilt coupled with fixed FOV will have large impacts on the visibility of each luminaire and the ability to discriminate multiple VLC/VLP signals.

The Line of Sight (LoS) optical channel DC gain is defined by

$$H_{DC}(\phi_i, \psi_i, d_i) = \frac{P_r^{(i)}}{P_t^{(i)}} = \frac{G_T(\phi_i) G_R(\psi_i)}{d_i^2}, \tag{1}$$

where $P_t^{(i)}$ and $P_r^{(i)}$ are, respectively, the power transmitted and received from the i-th transmitter. The transmitter gain (i.e., G_T) and the receiver gain (i.e., G_R) are defined

$$G_T(\phi) = \frac{m+1}{2\pi} \cos^m(\phi) \tag{2}$$

and

$$G_R(\psi) = \begin{cases} A\cos(\psi) & \psi < \Psi_C \\ 0 & else \end{cases} \tag{3}$$

respectively. For the examples within this paper, we model the Lambertian emission with order m and use a photodetector with area A and no filter or optical lens. The angle Ψ_C is the receiver's FOV and is dependent on the dimensions of the cone. When no cone is used, we have $\Psi_C = 90°$.

For signal transmission via Intensity Modulation with Direct Detection (IM/DD), conversion between the electrical and optical domains must be accounted for. Assuming the i-th transmitter is within the receiver's FOV, the amplitudes of the received and transmitted electrical signals are defined as follows:

$$\frac{A_y^{(i)}}{A_x^{(i)}} = \frac{C_T C_R (m+1)}{2\pi d_i^2} \cos^m(\phi_i) \cos(\psi_i), \tag{4}$$

where C_T and C_R are the proportionality constants that account for the fixed parameters within the system for a given scenario. C_T relates the range of the optical signal to the range of the drive signal $x(t)$. C_R accounts for any gain from receiver circuitry, the receiver area and its responsivity (A/W). These constants hold as long as the optical transmitter and receiver are both operating in their linear ranges. Note that we observe amplitude of sinusoidal signals in order to characterize the potential system performance within the linear range and in the presence of DC ambient light. The right hand side of Eq. (4) can also be used to relate maximum, minimum, or average of the transmitted and received signals.

Using this channel model and a system model based on the testbed's dimensions and layout, we can predict the signal strength from each luminaire at any receiver position and orientation. Ultimately, we aim to use this model to establish performance in the dynamic (mobile) case for any device operating within the lighting field. The physical system and the model differ in one important way: the model assumes point sources emitters, whereas in practice they are not. Moreover, the luminaires are asymmetrical, producing a rectangular pattern as desired for lighting. In spite of this assumption, the data predicted have good alignment with system measurements.

C. Data Collection

We measure the strength of signals originating at each of 15 luminaires within the lighting field. Each luminaire is configured to emit a unique carrier frequency. These are modulated using our SDR/USRP modified for VLC [4].

The receiver is the Thorlabs device mentioned earlier. The distance from the plane of the luminaires to the plane of receiver is 1.47 m. Various lenses and lens tubes are used to reduce or expand the field of view on the receiver. For the data set reported here, we use (*i*) a bare photo-detector (PD) without lens tube and (*ii*) a lens tube. The lens tube internal diameter at the PD is measured to be 25.64 mm and the length is 33.5 mm. Based on these dimensions, the FOV of the receiver is calculated to be 41.8°. Incident signals to the PD are captured at each position and orientation, using a custom script implemented in GnuRadio. The signals are recorded and subsequently processed to establish signal power at each frequency received.

Fig. 4 shows the receiver and servo mount used in the testbed for data collection. Translational and rotational data are collected by stepping the receiver through positions in the lighting field by incrementing X and Y coordinates. At each coordinate, the PD is rotated to render signal strengths

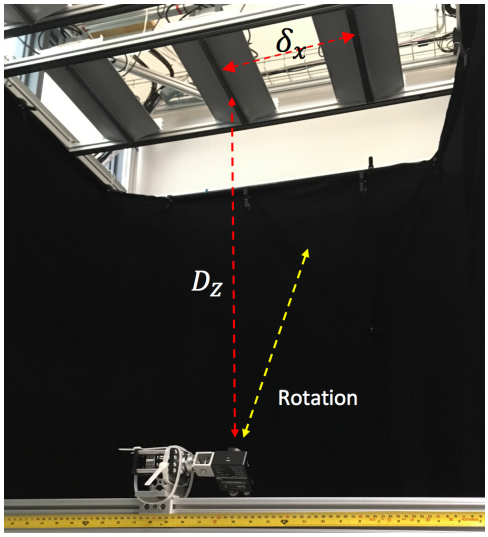

Fig. 4. Testbed Configuration

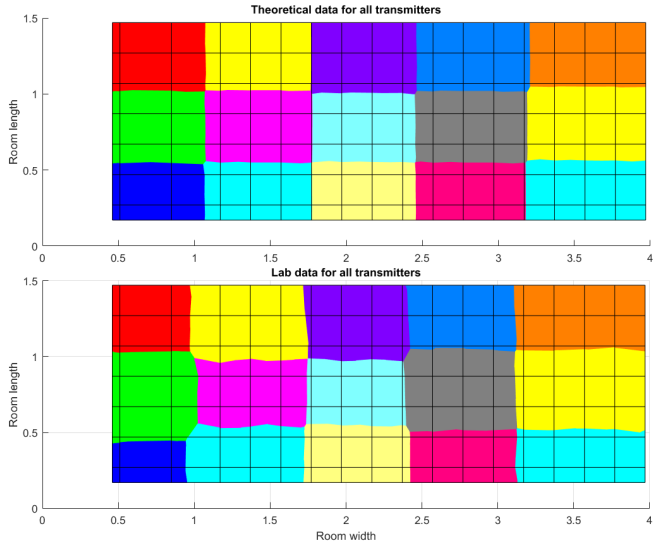

Fig. 5. Regions of Maximal Signal Strength at each XY position from (*top*) analytical model and (*bottom*) measurements.

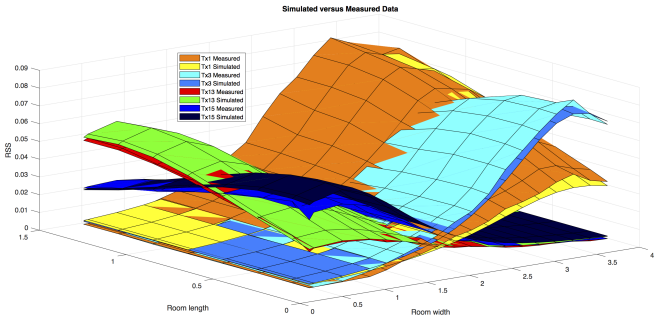

Fig. 6. Comparison of Measured vs. Predicted RSS Values Originating at Specific Luminaires.

received at angles of $\{0°, 15°, 30°, 45°\}$, where $0°$ represents the receiver pointing directly upward.

Data collection is facilitated by using a movable gantry that allows accurate positioning of the receiver in the XY plane. Orientation changes are realized by a servomechanism that cycles through different receiver angles. To isolate effects due to reflections and other ambient light, we wrapped the lighting field in black, non-reflective fabric.

D. Model Results

Fig. 5 and 6 are representative of the conformance of the model to the measured data. Fig. 5 illustrates the regions of maximum signal strength produced by the overhead luminaires as measured at all points in XY plane of the lighting field. The top graphic in Fig. 5 shows the model, whereas the bottom graphic shows measured data from the testbed. Each of these colored regions represents a clear delineation of the maximum signal to adopt in supporting design decisions in RSS-based VLP and handover algorithms. Similarly, Fig. 6 shows a comparison of RSS data generated from the analytical model, as compared against measured data. This example illustrates data collected without the lens tube. We notice that both measured and predicted (simulated) data have good alignment.

III. VLP RSS-Trilateration Analysis

In this section, we turn to interpreting data collected in the testbed and how it can be used to study the performance of VLP algorithms based on RSS. In particular, we focus on how RSS performance is impacted by occlusions, mobility (i.e., translational and rotational), and receiver optics. In relation to the optics, localization can be improved through redundancy in the number of luminaires with a LoS path to the receiver. However, this is contradictory to the use for communications where overlapping coverage can lead to interference in multi-user scenarios. To this end, we explore the impact of receiver optics on the location accuracy of a RSS-based VLP algorithm at various locations in the testbed environment.

A. RSS Based VLP Ranging

RSS-based VLP is a method that uses the relationship between a known transmitted signal strength and an estimated RSS to approximate range by solving for distance in the theoretical path loss model. RSS algorithms are widely used in the Radio Frequency (RF) domain. However, the optical channel's high dependence on relative orientation makes the VLP problem more challenging.

We first fix the height and rotation of the receiver in order to simplify the problem and limit the number of unknowns such that we can implement the system in our testbed with 15 transmitters. Setting the elevation angle as $\theta_{el} = 90°$, it implies that $\psi_i = \phi_i$ for all i.

We also remove the filter and lens so that $T_s(\psi) = 1$ for all ψ. When modeling no lens as $n = 1$ and $\Psi_C = 90°$, we find that $g(\psi) = 1$ in all cases since $0 \leq \psi \leq \Psi_C$ when $\theta_{el} = 90°$, and the receiver is located below the transmitters.

If we also define a fixed height that allows to compute a known vertical distance (i.e., D_z), we can define the relationship $\cos(\phi_i) = D_z/d_i$. Then, by replacing the cosine function in Eq. (4) with this ratio, we can solve for d_i.

Our RSS VLP algorithm relies on using a known, characterized signal and its channel model to estimate distance from signal loss. Other methods of positioning include Time-of-Arrival (ToA), Angle-of-Arrival (AoA), or Time-Difference-of-Arrival (TDoA). RSS positioning was chosen because it requires less hardware as compared to other systems (e.g., multiple receivers for AoA, a synchronized clock source for ToA, etc). RSS algorithms are largely used in other systems, including in the RF domain, because of its relative simplicity; however, signal occlusion and mobility present larger difficulties for the optics. To counter this, the photodiodes were kept at a fixed height and position. Each transmitted signal was a sine wave of a unique frequency transmitted from the luminaires from between 100 kHz to 800 kHz. Except for possibly over saturating the receiver photodiode, the high frequencies meant that there was little to no interference from the ambient light after measuring RSS through a Goertzel filter centered on the signal.

Using Eq. (4), we can solve for d_i to obtain the distance estimation i.e.,

$$d_i = \left[\frac{A_x^{(i)}}{A_y^{(i)}} C_T C_R \frac{m+1}{2\pi} (D_z)^m \right]^{\frac{1}{3}} \tag{5}$$

where D_z is the vertical distance between transmitters and the receiver. $C_T C_R$ is the constant proportionality that relates the input of the optical transmitter to the optical signal, the received optical signal to photodiode current, and any gain constants such as area or responsivity and was experimentally measured as a function of frequency for the range 100 kHz to 800 khz.

After estimating distances d_i from each transmitter to the receiver, multilateration is used to calculate position. First, a $[3 \times (N-1)]$ matrix $\mathbf{A}$ is constructed using the known coordinate positions relative to a reference point, i.e., luminaire 1. The estimated distances are used to construct another $[3 \times (N-1)]$ matrix $\mathbf{b}$, where N is the number of transmitters. Then, a least-squares solution of the equation $\mathbf{Ax} = \mathbf{b}$ is solved for $\mathbf{x}$.

$$\mathbf{A} = \begin{bmatrix} x_2 - x_1 & y_2 - y_1 & z_2 - z_1 \\ x_3 - x_1 & y_3 - y_1 & z_3 - z_1 \\ \vdots & \vdots & \vdots \\ x_N - x_1 & y_N - y_1 & z_N - z_1 \end{bmatrix}. \tag{6}$$

$$\mathbf{x} = \begin{bmatrix} x - x_1 \\ y - y_1 \\ z - z_1 \end{bmatrix} \tag{7}$$

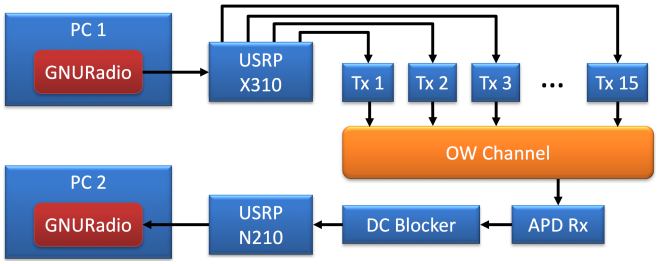

Fig. 7. Signal Chain for GnuRadio SDR System in Testbed

$$\mathbf{b} = \begin{bmatrix} \frac{1}{2}\left(d_1^2 + d_{1,2}^2 - d_2^2\right) \\ \frac{1}{2}\left(d_1^2 + d_{1,3}^2 - d_3^2\right) \\ \vdots \\ \frac{1}{2}\left(d_1^2 + d_{1,N}^2 - d_N^2\right) \end{bmatrix} \tag{8}$$

Since each luminaire is at the same height, the calculated z-value is always zero and is discounted (since the height is known). When accounting for signal occlusion and mobility, only the N_s smaller distances and therefore the stronger signals are used, where N_s is a pre-defined variable that is how many signals to use in multilateration. For multilateration to work, $N_s \leq 4$ and accuracy increases as N_s approaches N, and the solution is overly determined. However, this is a trade-off as with higher N_s values the chances of an occluded signal are higher.

Solving for $\mathbf{x}$ gives a location prediction for the receiver when $\mathbf{b}$ is calculated using the estimates of d_1 through d_N. Note that the transmitter height differences in the third column go to zero when the luminaires are located in the same z plane.

The software was implemented in GnuRadio as an out-of-tree module written in C++. GnuRadio provides a large library of standard blocks, including type converters, Fourier transforms and analysis, and GUIs that users can use to build flowgraphs. C++ is used for performance intensive operations while Python is used for rapid development. Two flowgraphs are used in the VLP system. The first is part of the transmitter setup drives output signals (fixed frequency sine waves) through multiple USRPs to modulate the 15 luminaires. The other receiver flowgraph performs RSS analysis and multilateration, saving the recorded signals and raw data for later analysis. The general signal chain is shown in Fig. 7.

B. Example Results

The RSS multilateration technique implemented in GnuRadio allows to both estimate the receiver position in real time on a GUI or to save RSS data for post processing. In either case we can manipulate the receiver position, orientation, and field of view, producing a great number of variants. Fig. 8 shows an example of the output of post processing of error estimates for an experiment using RSS data and six-lateration (i.e., using the six strongest RSS values in the field of view). The results show differences in performance between the X and Y dimensions clearly due to the asymmetry of the luminaires. We notice better performance in the Y dimension,

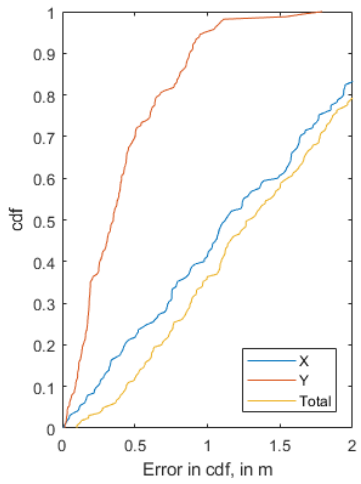

Fig. 8. CDF of Position Error using Six-Lateration.

which shows approximately 50% of the Y value estimates being accurate to within 50 cm. These results, although modest in terms of accuracy, illustrate the ability of the testbed to study the performance of the various VLP technique for indoor environments.

IV. VLC Handover in Dense Arrays

Similar to the study of VLP in the testbed, we seek to use the multiple luminaires to understand and design how to realize continuous coverage to mobile VLC devices in a dense environment.

In the lighting testbed, we are able to explore the effect of various outage conditions to determine the preferred handover technique, in order to maintain the service connectivity. In particular, we consider (*i*) out-of-range signal loss due to translational motion (i.e., when a device moves out of the access points coverage region), (*ii*) out-of-range signal loss due to rotational motion (i.e., when a device rotates such that the access point is no longer with the field of view), and (*iii*) signal loss due to obstruction (i.e., when the line-of-sight path between an access point and a static device is obstructed by a mobile obstruction).

A. System/Channel Model Predictions

For handover analysis, using the received power from the channel model, we are able to calculate the SNR throughout the testbed for data modulated through On-Off keying (OOK), i.e.

$$SNR = \frac{(RP_{tx}H_{DC})^2}{N_0 B} = \frac{\sigma_{sig}^2}{\sigma_n^2} \tag{9}$$

where R is the responsivity of the receiver, N_0 is the noise power spectral density, B is the receiver bandwidth, σ_{sig}^2 is the signal variance and σ_n^2 is the noise variance.

We assume a maximum bit error rate (BER) that we can allow in the system, i.e.

$$BER = Q(\sqrt{SNR}) \tag{10}$$

from which we can get the equivalent minimum SNR threshold that needs to be maintained for achieving the required BER.

B. Results

Our handover model assumes the receiver attempts to connect to the maximum available VLC signal. We show results for a wide FOV (no lens tube) and compare it to narrow FOV (having a lens tube on without any filter or lens in). It is worth noting that narrowing the FOV decreases the noise noticeably and gives overall better SNR/BER performance than the wide FOV, but of course we can achieve better overall performance by increasing the transmitted power in the system. We also show results for different receiver tilts and how tilting the receiver in opposite directions can show a mirror effect on the received signal strength.

Fig. 9 illustrates the impact of using a lens tube on the effective SNR at the receiver. Without a lens tube (top), the PD at the receiver is subjected to incident light from each of the 15 luminaires. These combine to raise the noise floor at the receiver. The graphic illustrates points in the XY plane that realize SNR values exceeding the BER value at the FEC limit of 10^{-3}. In contrast, the use of a lens tube isolates luminaires more proximal to the receiver, effectively reducing the receiver FOV. The result is broad access to higher SNR values throughout the lighting area. The use of the narrow FOV that the cone provides is clearly advantageous for improving VLC performance.

Fig. 10 shows a simulation of a user device transecting a diagonal of the lighting field. The top graphic shows a 60° tilt (30° from the normal), approaching from the right. As the device moves through the lighting field, luminares enter the FOV of the tilted receiver initially at high values, and fall away as the device moves farther into the array. The lower graphic illustrates the reverse direction, when a user enters from the left side and with a tilt in the opposite direction. The envelopes of these curves provide an indication of the peak SNRs attainable, and by which luminaire in the array. We can use this envelope as a basis for handover in a maximal SNR-based switching algorithm that is in development.

V. Conclusion

LiFi is an exciting new technology that is expected to be deployed initially at modest data rates in arrays supporting the lighting mission. We present our work on developing a testbed for studying VLC and VLP systems. The proposed model anticipates the use of multiple luminaires that are detected by a mobile receiver that can undergo changes in orientation and occlusions. The model is compared with experimental data collected in the testbed and shows good conformance for predicting received signal strength necessary for understanding the performance of RSS-based multilateration and for developing new algorithms for handover in multi-cell VLC.

With this work, we anticipate using the testbed and model to design new protocols that can operate with a range of mobility, device orientation, and interconnection with different network media.

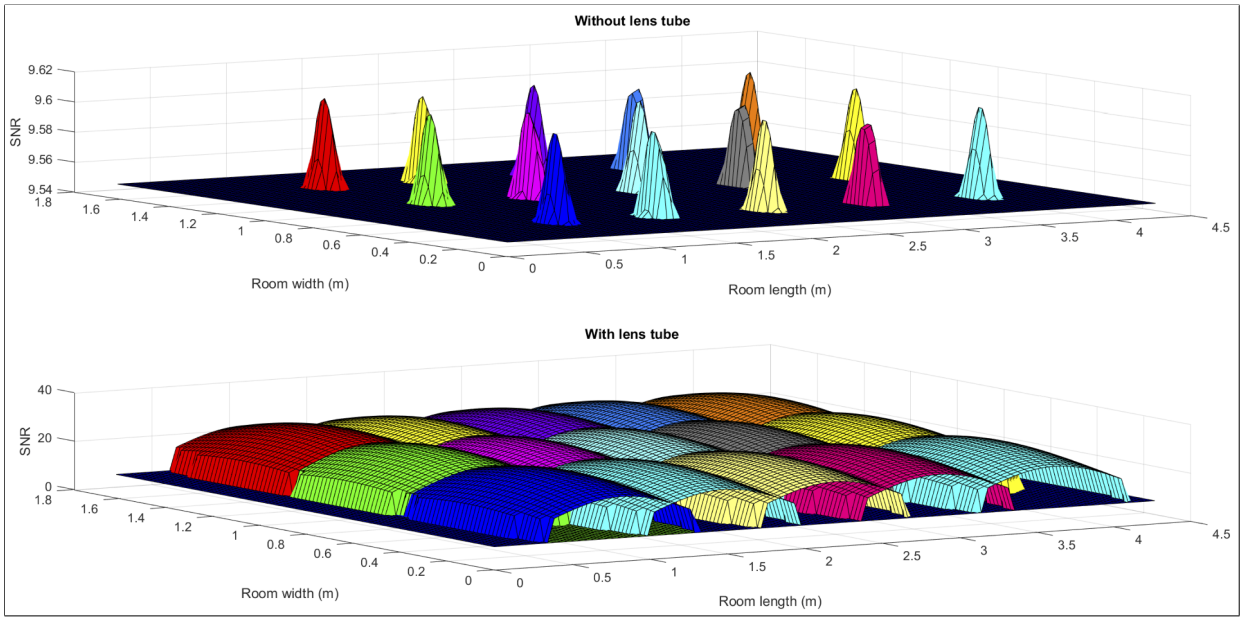

Fig. 9. Impact of Lens Tube on SNR in Lighting Array

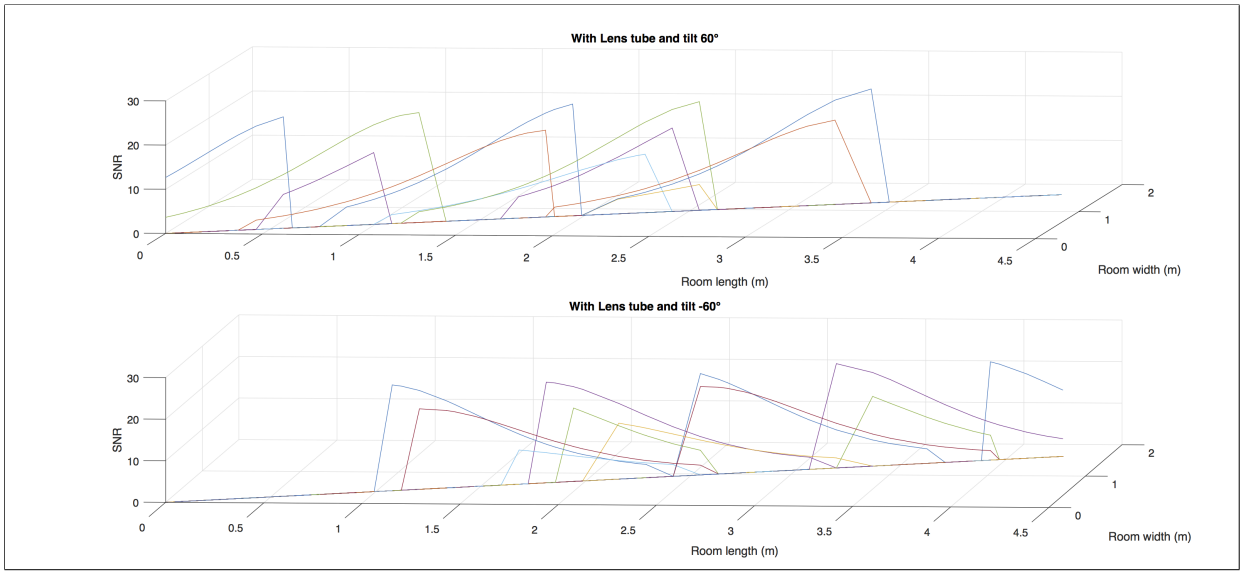

Fig. 10. Impact of Receiver Tilt with Lens Cone (Two Directions of Approach).

REFERENCES

[1] D. Tsonev, S. Videv, and H. Haas, "Light fidelity (li-fi): towards all-optical networking," *Proc.SPIE*, vol. 9007, pp. 9007 – 9007 – 10, 2014. [Online]. Available: http://dx.doi.org/10.1117/12.2044649

[2] B. Fahs, A. Chowdhury, and M. Hella, "A 12-m 2.5-gb/s lighting compatible integrated receiver for ook visible light communication links," *J. Lightwave Technol.*, vol. 34, no. 16, pp. 3768–3775, Aug 2016. [Online]. Available: http://jlt.osa.org/abstract.cfm?URI=jlt-34-16-3768

[3] A. Hussein and J. Elmirghani, "10 gbps mobile visible light communication system employing angle diversity, imaging receivers, and relay nodes," *IEEE/OSA Journal of Optical Communications and Networking*, vol. 7, no. 8, pp. 718 – 735, August 2015. [Online]. Available: http://eprints.whiterose.ac.uk/89032/

[4] M. Rahaim, A. Mirvakili, S. Ray, M. Hella, V. Koomson, and T. Little, "Software defined visible light communication," in *Wireless Communications Technologies and Software Defined Radio (SDR-WInnComm), Wireless Innovations Forum Conference on*, 2014.

[5] S. Shao, A. Khreishah, M. Rahaim, H. Elgala, M. Ayyash, T. Little, and J. Wu, "An indoor hybrid WiFi-VLC internet access system," in *2014 IEEE 11th International Conference on Mobile Ad Hoc and Sensor Systems (MASS)*, Oct 2014, pp. 569–574.